POLITECNICO DI TORINO
Repository ISTITUZIONALE

USER-FIRENDLY INTERFACE FOR TRAJECTORY LEARNING OF AN ASSISTIVE MOBILE MANIPULATOR

(Article begins on next page)

17 July 2024

USER-FRIENDLY INTERFACE FOR TRAJECTORY LEARNING OF AN ASSISTIVE MOBILE MANIPULATOR

Lorenzo Baglieri[0000−0002−5022−5326], Luigi Tagliavini[0000−0001−8925−0417], Andrea Botta[0000−0002−7272−7132], Giovanni Colucci[0000−0002−2996−9013], and Giuseppe Quaglia[0000−0003−4951−9228]

DIMEAS, Politecnico di Torino, corso Duca degli Abruzzi, 24, Torino, 10129, Italia
https://www.polito.it/
{lorenzo.baglieri, luigi.tagliavini, andrea.botta, giovanni_colucci, giuseppe.quaglia}@polito.it

ABSTRACT This paper presents a novel method to enable non-expert operators to drive a mobile manipulator and to teach new trajectories through interaction with the robotic arm. The paper describes how the generator of velocity reference is implemented. It takes as input the force applied by the user to the robotic arm and, through some post-processing, produces a velocity reference related to the input. The paper also investigates which input can be used as a reference signal and the post-processing done to obtain a velocity reference. A comparison between torque and force input is presented, explaining the reason that leads to the use of torque. The proposed method is useful to increase the number of people that can drive the mobile manipulator and reconfigure the trajectory. Although this method has been developed to increase the usability of the Paquitop platform among the medical staff in the hospital environment, the strength is that it can be implemented and used for all mobile manipulators that perform tasks of personal assistance.

KEYWORDS: Trajectory Learning, Omnidirectional Platform, Service Robotics, Mobile Manipulator, Robotic Arm.

1. INTRODUCTION

In the last decades, many researchers developed the theme of socially assistive robotics (SAR) developing a mobile platform to help fragile individuals with care and monitoring. In this context, the authors at Politecnico di Torino proposed an innovative pseudo-omnidirectional platform, named Paquitop [1],, which has high mobility in the plane of motion using conventional wheels. Based on this mobile platform, a lightweight mobile manipulator has been proposed. It is controlled by an embedded onboard computing module that coordinates the platform and the manipulator movements [2] to reach the desired position and perform the required tasks. The robotic platform is also provided with a LIDAR, a tracking camera and a state-of-art autonomous navigation algorithm, which combines the information from the two sensors and performs the navigation in a cluttered and unstructured environment, avoiding collision with static and dynamic obstacles. The autonomous navigation follows the preliminarily recorded waypoints to reach the desired position. Although in literature algorithms for autonomous exploration are available [3, 4] they are not useful to save new waypoints for further navigation. The remote control is the only way to explore a new environment and learn new paths, by the update of waypoints, but it requires an experienced and instructed user.

The Paquitop robotic platform, shown in Fig. 1.a, is designed to support the medical staff in hospitals. Its main activity is assisting bedridden patients by measuring vital parameters, bringing objects and giving them a Communication Interface. Some preliminary experimental campaigns in the transfusion department of Molinette Hospital of Turin have already proved the capacity of the mobile manipulator to navigate autonomously from the charging station to the bed and recognize patients [5]. The bed position was updated in the waypoints item with the remote control, but while the performed tasks can be always the same, the bed position can frequently change so it is fundamental to have a tool to easily update the path that the mobile manipulator has to follow.

This paper aims to make the drive of the mobile platform more intuitive and user-friendly and to increase the number of people that can easily teach a new path to the platform. Various examples of vehicles driven by hand gestures [6] or by gaze and speech [7] are shown in the literature. The novelties of the proposed concept are that the user guides the platform by giving a force input, to the robotic arm, and that are used the devices that are already installed on it. The joints measure the force of the user and the acquired information is post-processed in order to obtain a velocity reference command for the platform and to save the waypoints of a new trajectory.
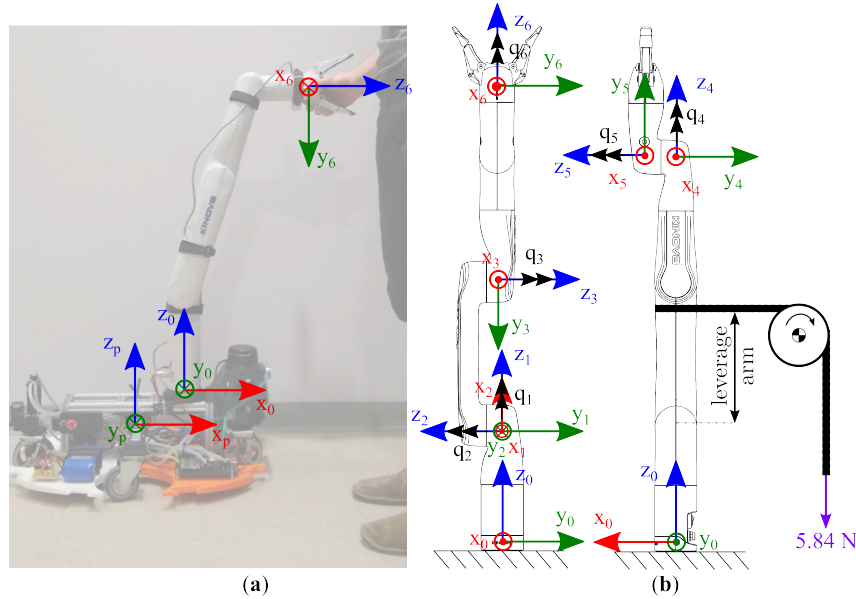

Fig. 1. (a) Reference frames of the robotic arm, of the mobile platform. The interaction between human beings and the robotic arm is displayed. (b) Reference frames of all the joints in the robotic arm mounted on the Paquitop platform according to the Denavit-Hartemberg convention. The experimental setup to measure the torque in the second joint is shown.

2. ANALYSIS OF THE ROBOTIC ARM FEEDBACK

The mobile base of the Paquitop platform permits pseudo-omnidirectional motion. Fig. 2 shows the two drive steering wheels that can have both different rotational and steering

speeds. The platform's low-level logic, implemented on a built-in microcontroller, transforms a velocity twist in angular velocities for the two traction motor wheels ($\dot{\theta}_r$ and $\dot{\theta}_l$) and two steering angles for the steering joints (δ_r and δ_l). The velocity twist is given with respect to the platform reference system shown in Fig. 2. It is a 6×1 vector that for the planar motion presents only the linear velocities along x and y and the angular velocity along z: $[v_x \ v_y \ 0 \ 0 \ 0 \ \omega_z]^T$.

Fig. 1.b shows the 6 degrees of freedom (DOF) robotic arm with the adopted reference frames, defined according to the Denavit-Hartemberg (D-H) convention, and the nomenclature. Fig. 1.a displays the user that interacts with the end effector of the robotic arm. The user's force applied to the end effector is decomposed along the reference frame of the robotic arm base. A simple and intuitive interaction can be obtained by linking the linear x and y velocity with the forces in the x and y direction and the angular velocity with the torque in the z-axis.
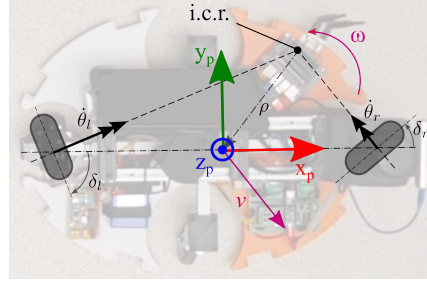

Fig. 2. The reference frame of the mobile platform with an example of omnidirectional velocity

2.1 Reliability of the measurements of the robotic arm

The robotic arm, designed for a collaborative environment, is provided by a software interface that makes the measured joint torques and forces exerted by the end effector available to the user. All the torque measurements of the robotic arm were tested by comparing the value of a known applied external torque with the absolute difference of the measure of torque taken before and after the application of the external torque. Fig. 1.b shows the experimental setup for the torque measurement in the second joint of the robotic arm. During the experiment, a force of 5.84 N was applied as far as possible to the second joint of the link between the third and the second joint. A cable pulley transmission guarantees the force is applied perpendicular to the link. A similar approach was used to test the remaining joint torque measurements, maintaining the same robotic arm position.

Table 1 contains the torque applied to each joint, the corresponding lever arm, the torque measured by the joint and its absolute and relative errors with respect to the applied torque. The measured torque is calculated as the absolute value of the difference between the torque measured by the joint with and without the applied force. The maximum error between the measured torques and the applied ones is in the second joint, while the maximum relative error is in the fourth one. On the other hand, the joints that scored the lowest relative error are the first, the third and the fifth. Regarding the absolute error, in addition to the previous one, also the fourth and the sixth show good results with small absolute errors. In

the majority of the joints is noticeable a measured torque lower than the applied one, this because of the friction effect of the robotic arm that helps in reacting to the external torque.

Table 1. Comparison between applied and measured torques

Joint	Lever arm $[cm]$	Applied $[Nm]$	Measured $[Nm]$	|Error| $[Nm]$	$\frac{\text{\|Error\|}}{\text{Applied}}$ %
1	5	0.29	0.3	0.01	3.45
2	30	1.75	1.5	0.25	14.29
3	24	1.40	1.3	0.10	7.14
4	4	0.24	0.2	0.04	16.67
5	18	1.05	1.1	0.05	5.25
6	6	0.35	0.3	0.05	14.28

2.2 The force feedback of the robotic arm

The software interface, typically used for the control of the applied force, measures the force that the user impresses on the robotic arm. Fig. 3 shows the forces and torques registered while a force is applied by the user's hand to the end effector in the negative x-axis direction with respect to the robotic arm base reference frame. The force has been calculated thanks to

$$\mathcal{F}_{user} = J^{-T}(\theta) \cdot (\tau_{user} + \tau_f + \tau_w) - \mathcal{F}_w = J^{-T}(\theta) \cdot \tau - \mathcal{F}_w \tag{1}$$

where $\mathcal{F}_{user}$ is the force that the user applies to the end-effector, $\mathcal{F}_w$ is the weight force applied by the robotic arm itself, J^{-T} is the inverse transposed Jacobian matrix, θ is the vector of the joint angular position and τ is the torque vector. The former can be decomposed in the gravity compensation torque τ_w, the friction torque τ_f and the torque τ_{user} to balance the user force in input.

$\mathcal{F}_w$ is estimated every time that the robot change position once the motion is completed. $\mathcal{F}_{user}$ generates a reaction in the robotic joints that apply τ_{user} to maintain the same position. When the $\mathcal{F}_{user}$ is no more present, the torque values can return to the original value or move to another equilibrium configuration with different values. As a consequence also the force measured by the robotic arm, that is a function of the torque applied to the joint, can change and produce the offset behavior shown by x Force and by the torque of the second joint in Fig. 3.

3. VELOCITY REFERENCES GENERATOR

Due to the fact that the torque offset measured at the second joint can assume values in the range [18.13%, 6.12%], acquiring reliable estimations of the input forces through the conventional method presented in section 2.2 is not possible. For this reason, the paper proposes a simplified method for the force input measurements that do not consider the torque measurement at joint 2. Fig. 4 points out how the generator of velocity references is implemented. The High-Level Logic of the onboard controller receives input from the measurement of the robotic arm and then post-process the signal to remove the offset in the measure. The post-processed signal is the mapping input signal to obtain a velocity reference signal for the platform. four different configurations have been taken into consideration in the experiment. The offset ranges depend on the joint position of the robotic arm, so Fig. 4 also highlights the dependence of the velocity reference generator on the configuration.
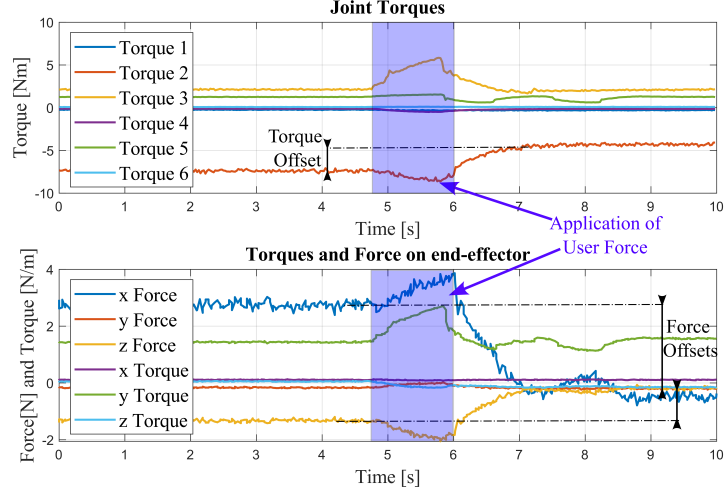
Fig. 3. Torque and force measurements do not have a fixed value at the rest condition. It depends also on the external force and the various combinations of torque values that can ensure the equilibrium of the robotic arm.

Due to the offsets in torque and force measurements, the Dead Band Remover performs the post-processing of the signals that are used as a reference of the generator. The following equation summarizes the algorithm to remove the offsets:

$$\tau_p = \begin{cases} \tau - \tau_{min} & \text{for } \tau \leq \tau_{min} \\ 0 & \text{for } \tau_{min} \leq \tau \leq \tau_{max} \\ \tau - \tau_{max} & \text{for } \tau \geq \tau_{max} \end{cases} \tag{2}$$

where τ_{min} and τ_{max} represent the minimum and the maximum value of the torque boundaries and τ_p is the post-processed signal. It is easier to collect the upper and lower boundary offset of the torques and check if each torque value is inside or outside the offset range. If τ is inside the offset, the post-processed value of the torque τ_p is zero, if τ is not included inside the offset, τ_p is decreased by the amount of the offset.
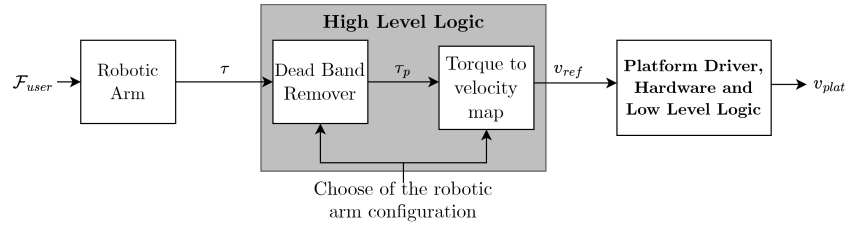

Fig. 4. Overall working scheme of the control system. It uses the torques input, does a proper post-processing and transforms the torques input into velocities output.

3.1 Configuration of the robotic arm

Fig. 5 shows the four configurations chosen to acquire the torque measurements from the user input force. The torques used as a reference change according to the selected configuration to better record the user's force. In the first and the second configurations the velocity along the x-axes depends on the fifth joint, the velocity along the y-axes depends on the sixth joint and the angular velocity along the z-axes depends on the fourth joint. While the third and fourth configurations present the same dependence between the y-axes and the sixth joint but the velocity along the x-axes is a function of the third joint and the angular velocity in the z-axes depends on the first joint.
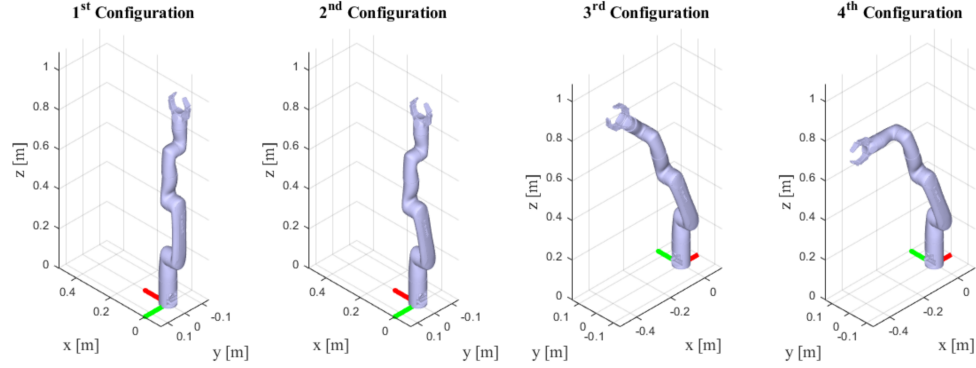
Fig. 5. The four different poses that are investigated in order to obtain the best $\mathcal{F}_{ext}$ measure. Joint angles in degree are: 1) [270, 0, 0, 0, 0, 0]; 2) [270, 10, 10, 0, 0, 0]; 3) [0, 20, 0, 90, -25, 0]; 4) [0, 20, 0, 90, -70, 0].

An experimental test was done to estimate the torque offsets and was repeated for each configuration. Fixed torque of 2 Nm was applied manually in both rotation directions at each joint. The torque measurement was repeated three times in each rotation direction. Table 2 shows the maximum and the minimum value recorded for each joint during the experimental test. From the table, it is possible to notice that the range of variation of the offset depends on the size of the motor and the configuration. The offset values recorded are used as τ_{min} and τ_{max} in (2).

3.2 Torque to velocity map

The map that transforms τ_p input to v_{ref} is a piece-wise function made of four parts. The first and the last ranges are represented by a linear equation. The second and third ranges are polynomials. The non-linearity around zero ensures a continuous junction between the two linear ranges and also a dead band where some little variations of τ_p do not produce unwanted v_{ref}. The generation of velocity reference selects from all the τ_p the torques that according to the configuration are used as velocity reference, as told before. The transformation map is defined as follows:

$$v_{ref} = \begin{cases} b_1\tau_p - b_0 & \text{if } \tau_p \leq -\tau_{plim} \\ a_5\tau_p^5 + a_4\tau_p^4 + a_3\tau_p^3 & \text{if } -\tau_{plim} \leq \tau_p \leq \tau_{plim} \\ b_1\tau_p + b_0 & \text{if } \tau_p \geq \tau_{plim} \end{cases} \tag{3}$$

Table 2. All the torque offsets measured in the different configurations. Joint angles in degree are: 1) [270, 0, 0, 0, 0, 0]; 2) [270, 10, 10, 0, 0, 0]; 3) [0, 20, 0, 90, -25, 0]; 4) [0, 20, 0, 90, -70, 0].

	1st Configuration			2nd Configuration		
Actuator	Min [Nm]	Max [Nm]	Range [Nm]	Min [Nm]	Max [Nm]	Range [Nm]
1	-0.8	0.9	1.7	-1.0	0.8	1.8
2	-2.5	3.3	5.8	1.0	3.0	2.0
3	-0.2	1.5	1.7	0.1	1.8	1.7
4	-0.1	0.1	0.2	-0.1	0.1	0.2
5	0.0	0.2	0.2	0.1	0.2	0.1
6	-0.4	0.4	0.8	-0.4	0.4	0.8

	3rd Configuration			4th Configuration		
Actuator	Min [Nm]	Max [Nm]	Range [Nm]	Min [Nm]	Max [Nm]	Range [Nm]
1	0.0	0.6	0.6	0.0	0.5	0.5
2	6.9	2.3	4.6	8.0	4.0	4.0
3	-1.8	-2.2	0.4	-2.0	-2.4	0.4
4	-0.2	0.0	0.2	-0.3	-0.1	0.2
5	-0.3	-1.0	0.7	-1.1	-1.3	0.2
6	-0.4	0.4	0.8	-0.4	0.4	0.8

where:

$$a_3 = 2\frac{5 \cdot v_{ref\,max} - 5 \cdot b_1\tau_{p\,max} + 3 \cdot b_1\tau_{p\,lim}}{\tau_{p\,lim}^3} \qquad b_0 = v_{ref\,max} - b_1\tau_{p\,max}$$

$$a_4 = -\text{sign}(\tau_p)\frac{15 \cdot v_{ref\,max} - 15 \cdot b_1\tau_{p\,max} + 8 \cdot b_1\tau_{p\,lim}}{\tau_{p\,lim}^4} \tag{4}$$

$$a_5 = 3\frac{2 \cdot v_{ref\,max} - 2 \cdot b_1\tau_{p\,max} + b_1\tau_{p\,lim}}{\tau_{p\,lim}^5} \qquad b_1 = \frac{v_{ref\,max} - v_{ref\,lim}}{\tau_{p\,max} - \tau_{p\,lim}}$$

where $v_{ref\,max}$ and $\tau_{p\,max}$ are the saturation value of torque and velocities. $v_{ref\,lim}$ and $\tau_{p\,lim}$ represent the changing point between the linear and polynomial behavior.

4. EXPERIMENTAL VALIDATION

The tests performed during the experimental validation evidenced how the velocity reference is built from torque signals and how the platform followed a trajectory using the generated velocity reference. Fig. 6 shows a trajectory done by driving the platform with the robotic arm and the torque input, with the velocity references that generated the platform movement.

5. CONCLUSION

The proposed method seems promising at enabling the non-experienced user to drive the robotic system. Through the acquisition and post-processing of the torque inputs, the high-level logic generates velocity references based on the user's force input. This application can be useful in a hospital environment where the platform should repeat always the same tasks but the positions of the patient could be updated easily with this method. Further studies will focus on automatizing the procedure to change the robot configuration and to save the pose of waypoints. To do so, different force feedbacks from the robotic arm or gesture recognition techniques applied to RGB-D camera images will be used.
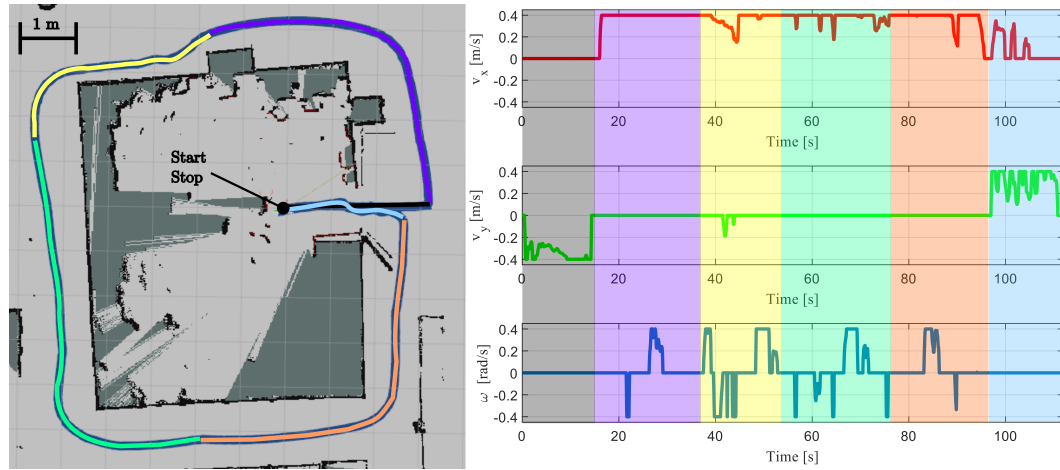
Fig. 6. The diagrams show the velocity references. The figure shows the trajectory performed by the mobile manipulator using the torque input and the velocity references.

REFERENCES

[1] Luca Carbonari, Andrea Botta, Paride Cavallone, and Giuseppe Quaglia. Functional design of a novel over-actuated mobile robotic platform for assistive tasks. In *International Conference on Robotics in Alpe-Adria Danube Region*, pages 380–389. Springer, 2020.

[2] Giovanni Colucci, Luigi Tagliavini, Luca Carbonari, Paride Cavallone, Andrea Botta, and Giuseppe Quaglia. Paquitop. arm, a Mobile Manipulator for Assessing Emerging Challenges in the COVID-19 Pandemic Scenario. *Robotics*, 10(3):102, 2021. Publisher: MDPI.

[3] Chao Cao, Hongbiao Zhu, Fan Yang, Yukun Xia, Howie Choset, Jean Oh, and Ji Zhang. Autonomous Exploration Development Environment and the Planning Algorithms. In *2022 International Conference on Robotics and Automation (ICRA)*, pages 8921–8928, May 2022.

[4] Andreas Bircher, Mina Kamel, Kostas Alexis, Helen Oleynikova, and Roland Siegwart. Receding Horizon "Next-Best-View" Planner for 3D Exploration. In *2016 IEEE International Conference on Robotics and Automation (ICRA)*, pages 1462–1468, May 2016.

[5] Luigi Tagliavini, Lorenzo Baglieri, Giovanni Colucci, Andrea Botta, Carmen Visconte, and Giuseppe Quaglia. D.O.T. PAQUITOP, an Autonomous Mobile Manipulator for Hospital Assistance. *Electronics*, 12(2):268, January 2023. Number: 2 Publisher: Multidisciplinary Digital Publishing Institute.

[6] Udara E. Manawadu, Mitsuhiro Kamezaki, Masaaki Ishikawa, Takahiro Kawano, and Shigeki Sugano. A hand gesture based driver-vehicle interface to control lateral and longitudinal motions of an autonomous vehicle. In *2016 IEEE International Conference on Systems, Man, and Cybernetics (SMC)*, pages 001785–001790, October 2016.

[7] Robert Neßelrath, Mohammad Mehdi Moniri, and Michael Feld. Combining Speech, Gaze, and Micro-gestures for the Multimodal Control of In-Car Functions. In *2016 12th International Conference on Intelligent Environments (IE)*, pages 190–193, September 2016. ISSN: 2472-7571.